J|A|C|S
COMMUNICATIONS

Published on Web 12/03/2003

A Solution-Phase, Precursor Route to Polycrystalline SnO_2 Nanowires That Can Be Used for Gas Sensing under Ambient Conditions

Yuliang Wang, Xuchuan Jiang, and Younan Xia*

Department of Chemistry, University of Washington, Seattle, Washington 98195

Received August 4, 2003; E-mail: xia@chem.washington.edu

One-dimensional (1D) nanostructures[1] have been a subject of intensive research due to their intriguing properties and unique applications. The simplest route to 1D nanostructures is probably the one that involves the use of an anisotropic crystal structure to induce the 1D growth.[2,3] The power of this method is, however, limited by the requirement that the target material must contain a chainlike structure. Here we demonstrate that the scope of this method could be extended to directly process a number of metal oxides into nanowires despite their isotropic structures.

Our initial demonstration was focused on SnO_2. In a typical synthesis, $SnC_2O_4 \cdot 2H_2O$ was mixed with poly(vinylpyrrolidone) (PVP) in ethylene glycol (EG), followed by refluxing at 195 °C for 3 h. Uniform nanowires with a mean diameter of ~50 nm and lengths up to 30 μm were formed as a white precipitate, which could be collected by centrifugation once the solution had cooled. Figure 1A shows the SEM image of a typical sample. A closer look by SEM and TEM (Figure S1) indicates that some of the wires could aggregate into bundles and thus appeared thicker in a low-magnification SEM or TEM image. Patterns recorded by X-ray powder diffraction (Figure S2) suggested that the as-synthesized nanowires were highly crystalline. When heated in air at 500 °C for 1 h, the nanowires could be transformed into crystalline SnO_2 (Figure S2B) without altering their 1D morphology.

Figure 1B shows an SEM image of the sample after calcination, indicating no morphological change. However, SEM (Figure 1C) and TEM (Figure 1D) imaging at high magnification revealed that each wire had been transformed from a dense structure with a smooth surface (Figure S1) into a highly porous structure consisting of interconnected nanocrystallites of ~5 nm in size. The SAED pattern (inset of Figure 1D) also confirmed that the nanocrystallites were made of rutile-phase SnO_2. This approach could also be extended to other metal oxides. Figure 1E shows an SEM image of In_2O_3 nanowires that were prepared by replacing $SnC_2O_4 \cdot 2H_2O$ with $In(O_2C_8H_{15})(O^iPr)_2$. In comparison with the SnO_2 nanowires shown in Figure 1C, a similar porous structure was also observed for the In_2O_3 nanowires. Figure 1F shows the SEM image of another example where nanowires of anatase TiO_2 were synthesized using a similar procedure, with $Ti(OBu)_4$ used as the starting material.

Figure 2 outlines a plausible mechanism responsible for the formation of nanowires in an isotropic medium. The key step was the oligomerization of tin glycolates, a process that has been discussed in several publications for the same or similar metal alkoxides.[4,5a−c] In the initial stage of refluxing, the oxalate groups of SnC_2O_4 were replaced gradually by ethylene glycol units through the formation of Sn−O− covalent and Sn ← OH coordination bonds. This hypothesis was supported by FT-IR studies (Figure S3), where we observed the disappearance of O−C═O vibrational bands (from oxalate group) and the appearance of CH_2− and C−OH bands (from ethylene glycol unit). As refluxing was continued, the tin glycolates underwent several steps of intermediate reactions as described in the scheme and eventually led to the formation of

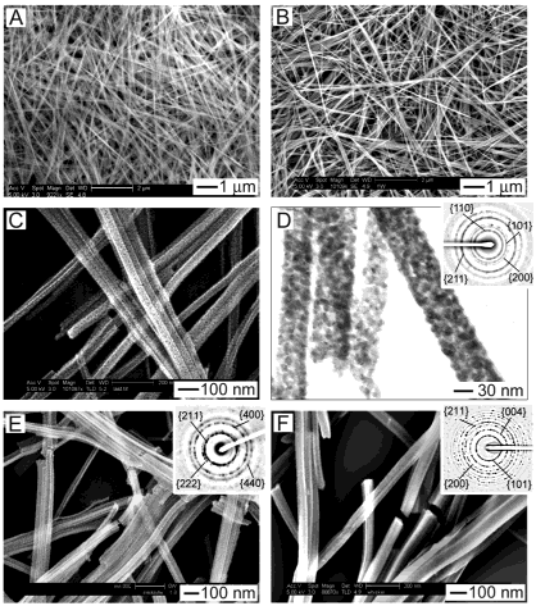

Figure 1. (A and B) SEM images of SnO_2 nanowires before (A) and after (B) calcination. (C and D) High-magnification SEM and TEM images of the calcined sample of SnO_2 nanowires. The inset shows a typical SAED pattern of the nanowires, which could be indexed to SnO_2. (E and F) SEM images and SAED patterns of nanowires made of In_2O_3 (E) and anatase TiO_2 (F) prepared using a similar procedure.

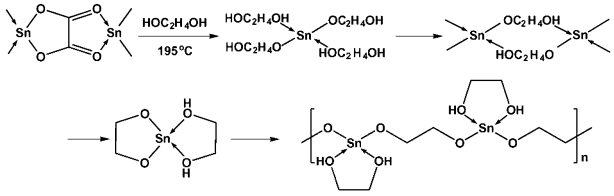

Figure 2. Schematic illustration of a proposed mechanism responsible for the formation of 1D nanostructures.

longer chains, which could further self-assemble into ordered bundles (i.e., nanowires) through van der Waals interactions. X-ray photoelectron spectroscopic (XPS) studies (Figure S4) indicated that the tin remained as Sn(II) in the precursor nanowires. Despite the insolubility associated with the final product, at least several dimeric and even tetrameric fragments have been identified in the supernatant solution by mass spectroscopy (Figure S5). Solid NMR spectrum (Figure S6) taken from precursor nanowires also support the polymeric structure shown in Figure 2. From TGA analysis (Figure S7), we observed a total of ~36% weight loss around 325 °C under N_2, which is close to the calculated value of 37.5% by considering the loss of two coordinated ethylene glycol and four carbon atoms (in the form of ethylene) for each repeating unit. For the linear chains, the repeating unit was found to have the following dimensions (Figure S2, $a \approx 10$ Å, $b \approx 3.6$ Å, and $c \approx 15$ Å) by

10.1021/ja037743f CCC: $25.00

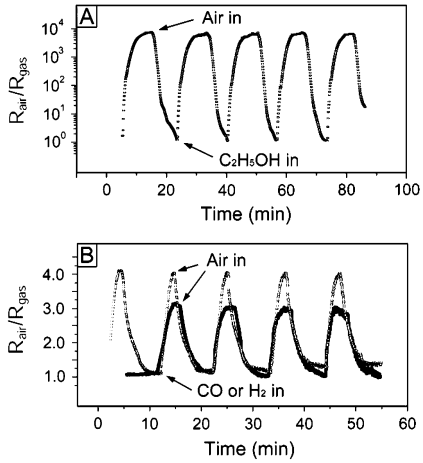

Figure 3. Changes in resistance for an SnO_2-based sensor when the surrounding gas was switched between (A) air and ~6% ethanol vapor in air as well as (B) air and 20 ppm CO (dashed line) or 500 ppm H_2 (solid line).

structural modeling (CHEM 3D Ultra 8.0, CambridgeSoft). For nanowires assembled from such linear building blocks, the crystal structure is yet to be determined. For now, it is assumed to be an orthorhombic one, with its lattice constants being the dimensions estimated for the repeating unit. The positions of diffraction peaks calculated using the ENDEAVOUR (version 1.2, Crystal Impact GbR) were in reasonable agreement with the experimental data (Figure S2A). XRD studies indicate that a similar mechanism was also shared by the systems that led to the formation of In_2O_3 and TiO_2 nanowires (Figure S8).

Prompted by their porous appearance, we suspected that these semiconducting nanowires must be useful in fabricating sensors. As an n-type semiconductor, SnO_2 has been extensively exploited in applications related to gas sensing. Most of these studies have focused on polycrystalline films made of small SnO_2 particles.[5d−f] Recent work indicated that 1D nanostructures (e.g., wires and belts) of SnO_2 could also be used to fabricate nanoscale sensors for various gases.[6] As limited by the surface areas of these nanostructures, high sensitivity and reversibility could only be achieved at an elevated temperature or by exposure to UV light. Here it was found that the SnO_2 nanowires prepared using the present method exhibited both high sensitivity and reversibility even under ambient conditions. Figure 3 shows the changes in resistance at room temperature when a thin-film sensor was exposed to several gaseous species at various concentrations (e.g., air-saturated ethanol taken from the pure liquid, 20 ppm CO, and 500 ppm H_2). For ethanol vapor (~6%, $V_{ethanol}/V_{air}$), we observed a total change of almost 8,000 times in resistance between the on and off states (Figure 3A). For CO and H_2 (Figure 3B), similar changes were also observed, albeit the magnitude was reduced to ~3 for H_2 and ~4 for CO due to the relatively low concentrations of these gases. In addition, it was found that such on and off responses could be repeated for more than 10 times without observing major changes in the signal.

For SnO_2-based sensors, the change in resistance is mainly caused by the adsorption and desorption of gas molecules on the surface of the sensing structure. Almost all previous studies involved the use of elevated temperatures or UV light to improve the molecular desorption kinetics and thus to help "clean" the surface.[5d−f] For the sensors described here, we believe that the high sensitivity and reversibility under ambient conditions can be attributed to the intrinsically small grain size and high surface-to-volume ratios associated with the polycrystalline nanowires.[7] For the conventional, film-type sensors based on SnO_2 particles, the surface-to-volume ratio is relatively low as a result of large grain sizes (~200 nm). Furthermore, only a thin layer of the film close to the surface can be activated during gas detection due to the dense structure of a compact film. In comparison, there exists a network of interconnected pores in our films, where the SnO_2 nanowires are randomly oriented to generate a highly porous structure. This network of pores enables both the analyte and the background gas to access all the surfaces of SnO_2 nanoparticles contained in the sensing unit. Different from sensors made of individual nanobelts of single crystalline SnO_2, the small grains of SnO_2 in our nanowires allowed the sensors to be operated in the most sensitive, grain-controlled mode. When the grain size is reduced to a scale comparable to the space-charge length (for SnO_2, this value is ~6 nm), the sensitivity could be exponentially enhanced.[8] The operation of such sensors at room temperature also helps to eliminate grain size changes that might occur as a result of thermal-induced sintering.

Acknowledgment. This work has been supported in part by an AFOSR-MURI grant on smart skins awarded to the UW and a fellowship from the David and Lucile Packard Foundation. Y.X. is a Camille Dreyfus Teacher Scholar (2002).

Supporting Information Available: Experimental procedures, high-magnification SEM and TEM images of the precursor nanowires, XPS, X-ray powder diffraction patterns, and FT-IR spectra of the nanowires before and after calcinations, a TGA curve, and a mass spectrum (PDF). This material is available free of charge via the Internet at http://pubs.acs.org.

References

(1) Xia, Y.; Yang, P.; Sun, Y.; Wu, Y.; Mayers, B.; Gates, B.; Kim, F.; Yan, H. *Adv. Mater.* **2003**, *15*, 353.
(2) $M_2Mo_6X_6$ (M = Li, Na; X = Se, Te): (a) Tarascon, J.; DiSalvo, F.; Chen, C.; Carrol, P.; Walsh, M.; Rupp, L. *J. Solid State Chem.* **1985**, *58*, 290. (b) Venkataraman, L.; Lieber, C. *Phys. Rev. Lett.* **1999**, *83*, 5334. (c) Messer, B.; Song, J.; Huang, M.; Wu, Y.; Kim, F.; Yang, P. *Adv. Mater.* **2000**, *12*, 1526.
(3) Trigonal Se and Te: (a) Gates, B.; Mayers, B.; Cattle, B.; Xia, Y. *Adv. Funct. Mater.* **2002**, *12*, 219. (b) Mayers, B.; Xia, Y. *J. Mater. Chem.* **2002**, *12*, 1875.
(4) (a) Fenton, D.; Gould, R.; Harrison, P.; Harvey, T.; Omietanski, G.; Sze, C.; Zuckerman, J. *Inorg. Chim. Acta* **1970**, *4*, 235. (b) Cocks, G.; Zuckerman, J. *Inorg. Chem.* **1965**, *4*, 592. (c) Honnick, W.; Zuckerman, J. *Inorg. Chem.* **1978**, *17*, 501. (d) Korb, G.; Levy, G.; Brini, M.; Deluzarche, A. *J. Organomet. Chem.* **1970**, *23*, 437. (e) Pommier, J.; Valade, J. *J. Organomet. Chem.* **1968**, *12*, 433. (f) Pommier, J.; Mendes, E.; Valade, J. *J. Organomet. Chem.* **1973**, *55*, C19. (g) Murakami, Y.; Matsumoto, T.; Yahikozawa, K.; Takasu, Y. *Catal. Today* **1995**, *23*, 383. (h) Mehrotra, R.; Gupta, V. *J. Organomet. Chem.* **1965**, *4*, 151. (i) Gaur, D.; Srivastava, G.; Mehrotra, R. *J. Organomet. Chem.* **1973**, *47*, 95. (j) Bradley, D.; Mehrotra, R.; Gaur, D. *Metal Alkoxides*; Academic: London, 1978; Chapter 4.
(5) (a) Scott, R.; Coombs, N.; Ozin, G. *J. Mater. Chem.* **2003**, *13*, 969. (b) Russell, G.; Henrichs, P.; Hewitt, J.; Grashof, H.; Sandhu, M. *Macromolecules* **1981**, *14*, 1764. (c) Barroso-Bujans, F.; Martinez, R.; Ortiz, P. *J. Appl. Polym. Sci.* **2003**, *88*, 302. (d) Camagni, P.; Faglia, G.; Galinetto, P.; Perego, C.; Samoggia, G.; Sberveglier, G. *Sens. Actuators, B* **1996**, *31*, 99. (e) Ihokura, K.; Watson, J. *The Stannic Oxide Gas Sensor;* CRC: Boca Raton, FL, 1994.
(6) (a) Kolmakov, A.; Zhang, Y.; Cheng, G.; Moskovits, M. *Adv. Mater.* **2003**, *15*, 997. (b) Law, M.; Kind, H.; Messer, B.; Kim, F.; Yang, P. *Angew. Chem., Int. Ed.* **2002**, *41*, 2405. (c) Comini, E.; Faglia, G.; Sberveglieri, G.; Pan, Z.; Wang, Z. *Appl. Phys. Lett.* **2002**, *81*, 1869.
(7) Favier, F.; Walter, E.; Zach, M.; Benter, T.; Penner, R. *Science* **2001**, *293*, 2227.
(8) (a) Shimizu, Y.; Egashira, M. *MRS Bull.* **1999**, *24*, 18. (b) Wu, N.; Wang, S.; Rusakova, I. *Science* **1999**, *285*, 1375. (c) Dieguez, A.; Romano-Rodriguez, A.; Morante, J.; Kapler, J.; Barsan, N.; Gopel, W. *Sens. Actuators, B* **1999**, *60*, 125.

JA037743F